Single Cl⁻ Channels Activated by Ca²⁺ in *Drosophila* S2 Cells Are Mediated By Bestrophins

Li-Ting Chien, Zhi-Ren Zhang, and H. Criss Hartzell

Department of Cell Biology and Center for Neurodegenerative Disease, Emory University School of Medicine, Atlanta, GA 30322

Mutations in human bestrophin-1 (*VMD2*) are genetically linked to several forms of retinal degeneration but the underlying mechanisms are unknown. Bestrophin-1 (hBest1) has been proposed to be a Cl⁻ channel involved in ion and fluid transport by the retinal pigment epithelium (RPE). To date, however, bestrophin currents have only been described in overexpression systems and not in any native cells. To test whether bestrophins function as Ca²⁺-activated Cl⁻ (CaC) channels physiologically, we used interfering RNA (RNAi) in the *Drosophila* S2 cell line. S2 cells express four bestrophins (dbest1–4) and have an endogenous CaC current. The CaC current is abolished by several RNAi constructs to dbest1 and dbest2, but not dbest3 or dbest4. The endogenous CaC current was mimicked by expression of dbest1 in HEK cells, and the rectification and relative permeability of the current were altered by replacing F81 with cysteine. Single channel analysis of the S2 bestrophin currents revealed an ∼2-pS single channel with fast gating kinetics and linear current–voltage relationship. A similar channel was observed in CHO cells transfected with dbest1, but no such channel was seen in S2 cells treated with RNAi to dbest1. This provides definitive evidence that bestrophins are components of native CaC channels at the plasma membrane.

INTRODUCTION

Age-related macular degeneration (ARMD) is one of the most common causes of blindness (Penfold et al., 2001), but its underlying mechanisms are not known. Although both genetic and environmental factors contribute to the pathogenesis of ARMD, some other forms of macular degeneration are inherited in a Mendelian fashion (Hartzell et al., 2005b). For example, Best vitelliform macular dystrophy (BVMD) (Godel et al., 1986) is linked to over 85 mutations, many of which are dominant, in the bestrophin-1 gene (*VMD2*) (Marquardt et al., 1998; Petrukhin et al., 1998; White et al., 2000; Weber and Krämer, 2002; Hartzell et al., 2005b; Strauss, 2005). Mutations in *VMD2* are also associated with a small fraction of cases of adult onset vitelliform macular dystrophy (Allikmets et al., 1999; Krämer et al., 2000) and abnormal splice variants of *VMD2* are associated with autosomal dominant vitreoretinochoroidopathy (Yardley et al., 2004).

A defect in epithelial ion transport is thought to underlie BVMD because its hallmark feature is a decreased slow light peak in the electrooculogram (EOG) (Deutman, 1969; Cross and Bard, 1974; Wajima et al., 1993). Experiments in chicken, cat, and gecko show clearly that the light peak is caused by a Cl⁻ conductance in the basolateral membrane of the retinal pigment epithelium (RPE) (Gallemore et al., 1997).

The light peak is blocked by the Cl⁻ channel blocker DIDS, the reversal potential of the light peak equals E_{Cl}, the reversal potential of the light peak changes in concert with E_{Cl}, and the relative Cl⁻ conductance increases during the light peak. Because bestrophin-1 immunoreactivity is found basolaterally in RPE cells (Marmorstein et al., 2000; Bakall et al., 2003), the simplest hypothesis is that BVMD is caused by a defect in the basolateral RPE Cl⁻ channel that is mediated by bestrophin-1 (hBest1).

Strong support for this hypothesis was provided by the demonstration by Sun et al. (2002) that hBest1 and other bestrophins induce Cl⁻ currents when overexpressed in HEK cells. Furthermore, they showed that several of disease-causing mutations in hBest1 produce currents in HEK cells that are considerably smaller than normal (Sun et al., 2002). The bestrophins that have been studied are dependent on Ca²⁺ in the physiological range (Qu and Hartzell, 2003, 2004; Qu et al., 2004). Further evidence that bestrophins are Cl⁻ channels was provided by the demonstration that mutations in both hBest1 and mBest2 alter the relative anion conductance and permeability of the currents and change their sensitivity to cysteine-reactive reagents (Tsunenari

---

Abbreviations used in this paper: BVMD, Best vitelliform macular dystrophy; CaC, Ca²⁺-activated Cl⁻; EOG, electrooculogram; hBest1, bestrophin-1; RPE, retinal pigment epithelium.

Correspondence to Criss Hartzell: criss.hartzell@emory.edu

et al., 2003; Qu and Hartzell, 2004; Qu et al., 2004, 2006a). The ability to change bestrophin selectivity by mutations provides good evidence that bestrophin is responsible for forming the channel pore (Pusch, 2004).

Despite these findings, the idea that hBest1 is an epithelial Cl^- channel has remained in doubt. The fact that several mutations in *VMD2*, like A243V, cause late-onset vitelliform macular degenerations that are not accompanied by EOG abnormalities (Kramer et al., 2000; Seddon et al., 2001, 2003; Pollack et al., 2005; Renner et al., 2005) has suggested that BVMD may not be caused by Cl^- channel dysfunction (Yu et al., 2006). An alternative hypothesis, that bestrophin is a regulator of voltage-gated Ca^{2+} channels, has been proposed by Marmorstein et al. (2004, 2006) and Rosenthal et al. (2005). Overexpression of hBest1 in RPE-J cells causes a shift in the voltage dependence of activation of L-type voltage-gated Ca^{2+} currents and changes their activation and deactivation kinetics (Rosenthal et al., 2005). Furthermore, overexpression of wild-type or dominant-negative bestrophins in rats does not have the expected effects on the EOG if bestrophin were functioning as a basolateral RPE Cl^- conductance (Marmorstein et al., 2004) and RPE cells from mBest1 knockout mice have normal Cl^- currents (Marmorstein et al., 2006). These findings have led these investigators to conclude that mBest1 is not involved in generating the light peak. Rather, they propose that bestrophin modulates the light peak by altering the voltage dependence of Ca^{2+} channels. Although the possibility might be considered that the light peak and its

ionic mechanisms differ in different species (compare, for example, Linsenmeier and Steinberg [1982] and Marmorstein et al. [2006]), the Cl^- channel hypothesis and the Ca^{2+} channel regulator hypothesis for bestrophin are not mutually exclusive. CFTR, for example, is a Cl^- channel that regulates a wide variety of different channels and transporters (Mehta, 2005).

Additional reasons to worry whether bestrophins are Ca^{2+}-activated Cl^- (CaC) channels are the findings that expressed bestrophin currents differ from native CaC currents (Pusch, 2004) and that mutations in mBest2 actually have somewhat unimpressive effects on anion selectivity (Qu et al., 2006a). These findings may suggest that the currents induced by bestrophin overexpression might be due to up-regulation of endogenous Cl^- channels. Up-regulation of endogenous Cl^- channels is a common response to overexpression of a variety of membrane proteins in *Xenopus* oocytes (Attali et al., 1993; Shimbo et al., 1995; Tzounopoulos et al., 1995). This has resulted in controversy about a variety of candidate Cl^- channels (Clapham, 1998; Jentsch et al., 2002; Hartzell et al., 2005a). For example, CLCA proteins have been proposed to be CaC channels (e.g., Cunningham et al., 1995; Yamazaki et al., 2005), but the prevailing view is that CLCAs are not Cl^- channels (Jentsch et al., 2002; Eggermont, 2004), partly because some CLCAs are secreted proteins (Gibson et al., 2005). This problem in unambiguously identifying Cl^- channels has arisen because it is difficult to separate endogenous and expressed currents; different Cl^- currents are often biophysically similar and very few specific blockers exist. The observation that wild-type mBest4 and hBest3 produce negligible Cl^- currents in a physiological voltage range when expressed in HEK cells raises additional questions about their role as Cl^- channels (Qu et al., 2006b).
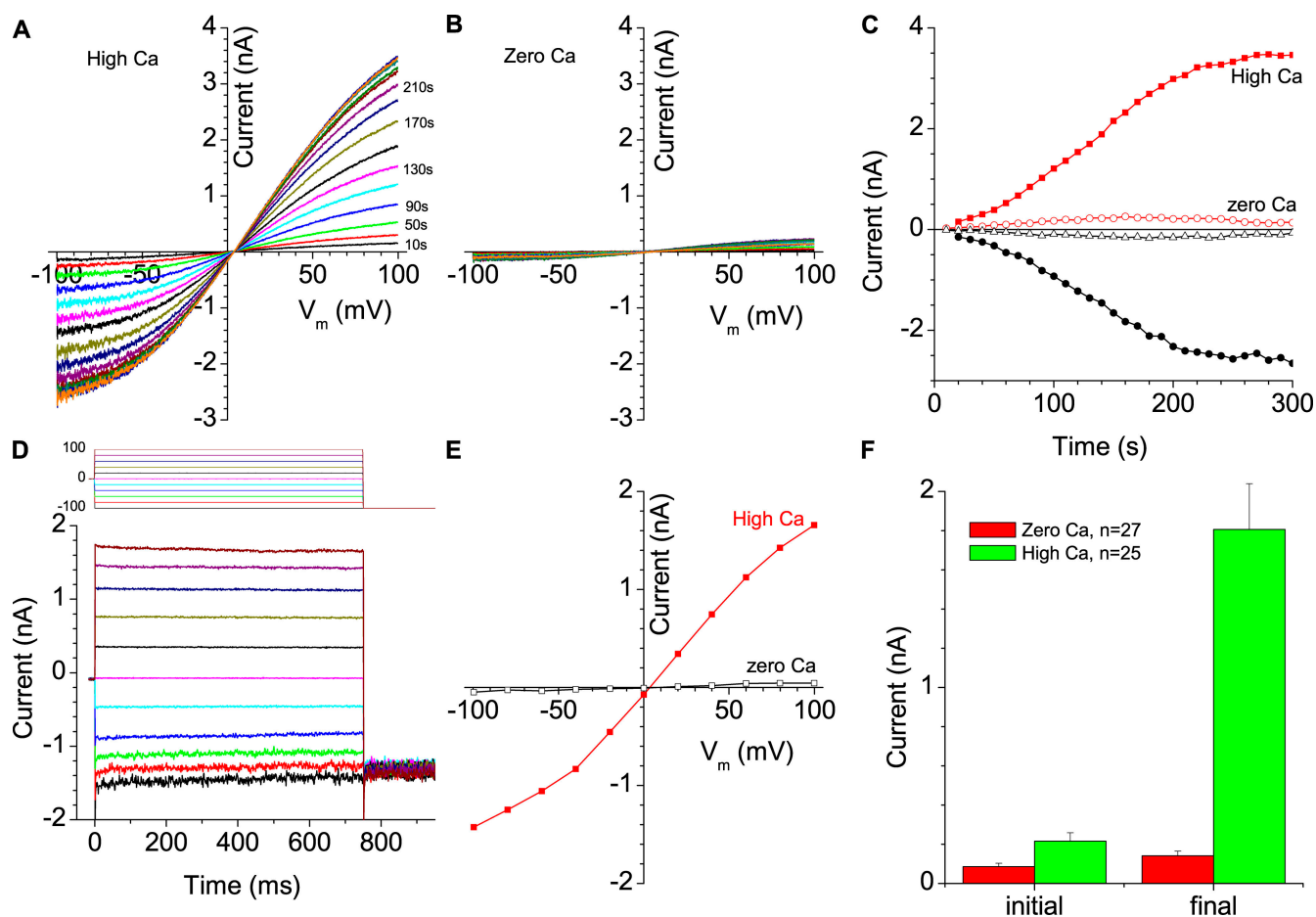
Figure 1. Endogenous *Drosophila* S2 cell chloride currents. (A–C) Time-dependent activation of a Cl⁻ current with (A) high or (B) zero intracellular Ca²⁺. Current–voltage relationships were recorded by voltage ramps at 10-s intervals after establishing whole-cell recording. (C) Current amplitudes with time after patch break at +100 mV (red) and −100 mV (black) for high Ca²⁺ (solid symbols) and 0 Ca²⁺ (open symbols). (D) Current traces in response to voltage steps recorded after the currents had reached their peak (>5 min after patch break). (E) Steady-state current–voltage relationship in high Ca²⁺ (solid symbols) and 0 Ca²⁺ (open symbols). (F) Average current amplitudes at +100 mV at the onset of whole cell recording (Initial) and after the currents have reached a steady state (final) in high (green) and 0 (red) Ca²⁺.

At least part of the uncertainty surrounding bestrophin function exists because an endogenous bestrophin-associated current has not yet been described in any cell type. We have used *Drosophila* S2 cells to test whether bestrophins function as CaC channels natively and have characterized the single channel properties of these channels. These findings strongly support the conclusion that bestrophins are CaC channels.

MATERIALS AND METHODS

Solutions

Drosophila S2 cells were cultured in Schneider's *Drosophila* Medium (GIBCO BRL) with 10% heat-inactivated FBS, 50 U/ml penicillin, and 50 μg/ml streptomycin in air at 22–24°C. HEK-293 cells and CHO cells (American Type Culture Collection) were cultured in Eagle's Minimum Essential Medium with ʟ-glutamine (Cellgro Co.), 10% heat-inactivated FBS (GIBCO BRL), and 50 U/ml penicillin and 50 μg/ml strepto-

mycin (GIBCO BRL) in 5% CO₂/95% O₂ at 37°C. Transfection was done as described by Qu et al. (2004). The "zero" Ca²⁺ intracellular solution used for patch clamping S2 cells contained (in mM) 143 CsCl, 8 MgCl₂, 10 EGTA-NMDG, and 10 HEPES, pH 7.3 (NaOH) (free Ca < 20 nM). The "high" Ca²⁺ (4.5 μM free) intracellular solution was the same, except 10 mM EGTA-NMDG was replaced by 10 mM Ca-EGTA-NMDG. The Ca-EGTA-NMDG stock was prepared as described previously (Qu and Hartzell, 2000) according to Tsien and Pozzan (1989) and was estimated to have ∼4.5 μM free Ca²⁺. The external solution used for patch clamp recording of S2 cells contained (in mM) 150 NaCl, 2 CaCl₂, 1 MgCl₂, 10 HEPES (pH 7.3 with NaOH), 15 sucrose, and 10 glucose. Osmolarity was adjusted with water or sucrose to 320 mOsM. For inside-out excised patch experiments, the patch pipet contained (in mM): 143 CsCl, 8 MgCl₂, 10 EGTA, 10 HEPES, pH 7.3. The bath (cytosolic) was either the same as the pipet solution (zero Ca) or contained a 10 mM mixture of Ca-EGTA and EGTA to make the desired free Ca concentration. In addition, the bath solution also usually contained 3 mM ATP. The standard pipette solution for HEK293 recording contained (in mM) 146 CsCl, 2 MgCl₂, 5 Ca-EGTA, 8 HEPES, 10 sucrose, adjusted to
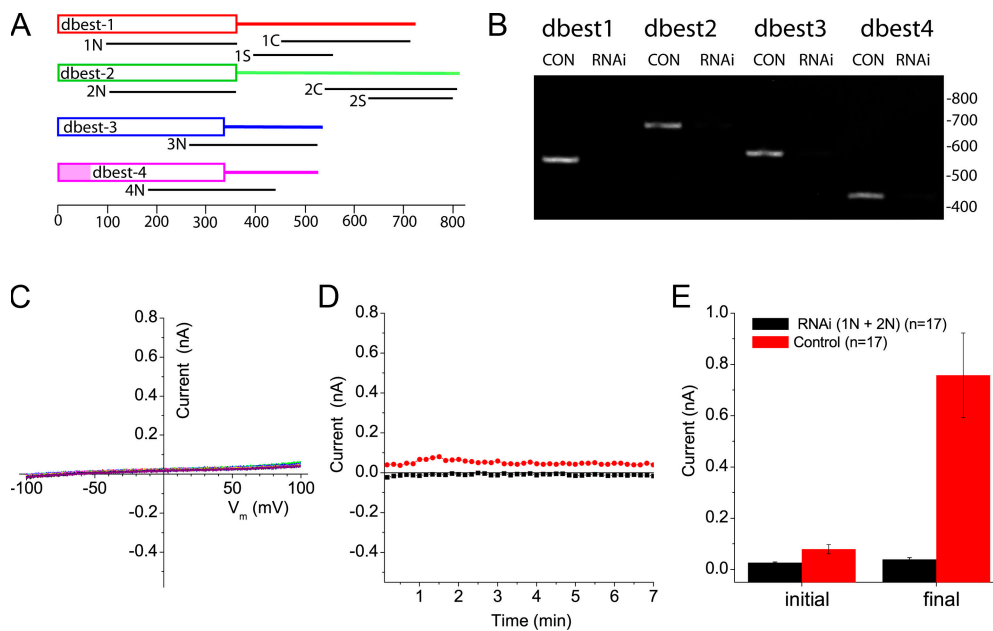
Figure 2. RNAi inhibition of dbest expression and CaC currents. (A) RNAi strategy. The conserved N-terminal regions of the four dbests are shown as boxes and the variable C-terminal regions shown as lines. The ruler shows amino acid number. The location of the RNAi constructs are shown by black lines below the dbests. (B) Expression of dbests by RT-PCR in cells treated with noninterfering dsRNA (CON) or a mixture of 1N and 2N RNAi (RNAi). Experiment was repeated three times. (C) Current–voltage relationship of RNAi-treated cell (superimposed traces spanning 6 min after patch break). (D) Time course of current activation in RNAi-treated cell after patch break. (E) Average current amplitudes at +100 mV immediately after patch break (initial) or after ∼5 min (final) for cells treated with control dsRNA (red) and 1N+2N RNAi (black).

pH 7.3 with NMDG as described previously (Qu and Hartzell, 2004). HEK-293 extracellular solution contained 140 NaCl, 5 KCl, 2 CaCl$_2$, 1 MgCl$_2$, 15 glucose, and 10 HEPES (pH 7.4 with NaOH). Osmolarity was adjusted to 304 mOsM. Cl$^-$ currents would be expected to have reversal potentials near zero with these solutions, while cation currents would have extreme nonzero reversal potentials. Cells exhibiting nonzero reversal potentials were discarded.

Electrophysiology

Patch-clamp was performed at room temperature (22–24°C). Fire polished pipets pulled from borosilicate glass (Sutter Instrument Co.) had resistances of 2–3 MΩ for whole-cell and 5–9 MΩ for single-channel recording when filled with intracellular solution. For whole-cell recording, cells were usually voltage clamped with 1-s duration ramps from −100 to +100 mV run at 10-s intervals or 750-ms voltage steps from −100 mV to +100 mV in 20-mV increments. Whole cell recording data were filtered at 2–5 kHz and sampled at 5–10 kHz by an Axopatch 200A amplifier controlled by Clampex 8.2 via a Digidata 1322A data acquisition system (Axon Instruments Inc.). For single channel recording, pipets were coated with Sylgard, recordings were obtained with an Axopatch 200B amplifier, and data were filtered at 5–10 kHz and sampled at 20–50 kHz. In all cases, sampling was at least twice the filtering frequency. For analysis, single channel records were filtered digitally at 200 Hz with an 8-pole Bessel filter. Data were analyzed using pClamp 9 software and Origin 7.0 as described by Qu et al. (2004). Data are expressed as mean ± SEM.

Cloning *Drosophila* Bestrophin cDNAs

The sequences of the *Drosophila* bestrophins used in this study agreed with Genbank/EMBL/DDBJ sequences for dbest1 (AY061546), dbest2 (BT010012), dbest3 (AAF49648), and dbest4 (AAF49649). dbest1 and dbest2 full-length cDNAs were purchased from *Drosophila* Gene Collection (Lawrence Berkeley National Laboratory). The open reading frames were amplified

by PCR and subcloned into the KpnI (5′) and NotI (3′) sites of pcDNA3.1 and sequenced.

RNA Interference

dsRNA was synthesized from dbest cDNAs. Control dsRNA was prepared from mBest2 intron 9. PCR primers (Table I) consisted of bestrophin gene-specific sequences with the T7 promoter sequence added to the 5′ ends (Van Gelder et al., 1990). Each primer was BLASTed against the *Drosophila* nucleotide database (NCBI) to ensure specificity. The PCR products were amplified with Pfx DNA polymerase (Invitrogen), gel-purified (QIAquick gel extraction kit, QIAGEN), and used for in vitro RNAi synthesis (mMESSAGE mMACHINE high yield capped RNA transcription kit, Ambion). RNAs were heated to 65°C for 10 min and annealed by slowly cooling to room temperature. For RNAi transfection, 10^6 adherent S2 cells in a 35-mm Petri dish were washed twice with serum-free medium and incubated with 40 μg of dsRNA in 1 ml of serum-free medium for 30 min at room temperature. 2 ml of medium containing serum was then added and the cells cultured for 2–6 d.

Reverse Transcriptase PCR

The efficiency of gene silencing by RNAi was evaluated by reverse transcriptase PCR (RT-PCR). Total RNA was purified by the Trizol (Invitrogen) method. Bestrophin gene-specific primers were designed to span exon/exon boundaries to ensure that genomic DNA was not amplified (Table II). RT- PCR was conducted using SuperScript III One-Step RT-PCR with Platinum Taq (Invitrogen). PCR band densities were quantified using an AlphaImager Imaging System (Alpha Innotech). Each PCR band was excised, gel-purified, and cloned into pCRII-TOPO (Invitrogen) for sequencing.

Western Blot

Antibodies were raised in rabbits against amino acids 440–718 of dbest1 with (His)$_6$ tags. The construct for the His-tagged dbest1 (440–718) was made by amplifying the dbest1 nucleotide

sequence encoding amino acids 440–718 using Pfx polymerase and primers to which EcoRI (forward) and NotI (reverse) restriction sites had been added. The PCR product was then subcloned into EcoRI and NotI sites of pET28a (Novagen). Protein expression was induced in BL21 *Escherichia coli* by IPTG, the bacteria were lysed with Bug Buster Protein Extraction Reagent (Novagen), and the His-tagged protein purified by chromatography on a Ni-NTA-His bind affinity column (Novagen). For Western blot, a crude membrane fraction of S2 cells was separated by SDS-PAGE on 10% Tris-HCl polyacrylamide gels and blotted to PDVF membrane. The antibodies were used at 1:5,000 dilution and detected by enhanced chemiluminescence (Super Signal, Pierce Chemical Co.). The antibodies did not recognize a band in the dbest1 knockout fly (*dbest1^1-2* and rescued λ5; *dbest1^1-2* lines were obtained from G. Mardon, Baylor College of Medicine, Houston, TX).

RESULTS

An Endogenous CaC Current in S2 Cells

Drosophila S2 cells express an endogenous CaC current (Fig. 1). When S2 cells were whole-cell patch clamped with either 0 Ca^{2+} (<20 nM free) or high Ca^{2+} ($\sim$4.5 μM) in the intracellular (pipet) solution, the currents observed with voltage ramps immediately after breaking the patch to initiate whole-cell recording were small, on average <250 pA ($n = 52$) at $+100$ mV. When the pipet contained high [Ca^{2+}], the current ran up after patch break (Fig. 1, A, C, and F) with a half-time of $\sim$2 min and reached a plateau that was on average 17.1 ± 3.2-fold (mean $\pm$ SEM, $n = 25$) greater than the initial current. The mechanisms for the run-up remain unknown, but preliminary data suggest phosphorylation might be involved. The run-up was accelerated when Mg-ATP was included in the internal solution, and the run-up was blocked by staurosporin (unpublished data). The external solution contained glucose, so that the cell was capable of synthesizing ATP. In contrast, when the pipet solution contained 0 Ca^{2+}, the currents remained stable after patch break (Fig. 1, B, C, and F). In some cells that were patched with zero Ca^{2+} pipet solution, the currents ran up for a short time and then ran down. The reason for this transient run-up is not known, but may be due to a spike of cytosolic Ca^{2+} associated with making or breaking the membrane patch. The currents stimulated by intracellular Ca^{2+} were carried by Cl^- ions, because they reversed near E_{Cl} (Fig. 1). The currents were unaffected by replacement of cations with $NMDG^+$ and replacement of extracellular Cl^- with SO_4^{2-} abolished outward currents (unpublished data).

The currents recorded with high intracellular Ca^{2+} did not show any significant time-dependent activation or inactivation in response to voltage steps (Fig. 1, D and E). The currents had small voltage dependence at the extremes of the voltage range, which gave the I-V relationship a characteristic "S" shape (Fig. 1, A and E).
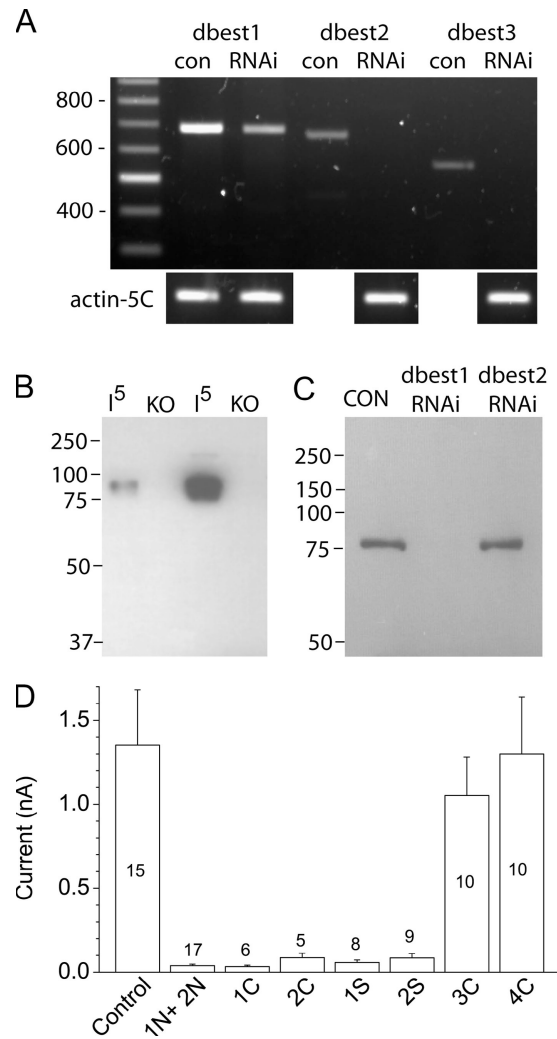

Figure 3. Specific RNAi inhibition of S2 CaC currents. (A) Quantitation of dbest expression by RT-PCR in cells treated with noninterfering dsRNA (con) or specific RNAi to dbest1 (1C, 679 bp), dbest2 (2C, 665 bp), or dbest3 (3C, 565bp). The actin-5C bands (426 bp) in the bottom panel show equal loading. These bands were obtained by RT-PCR of aliquots of the same RNAs used for the bestrophin RT-PCR in the top panel. The actin-5C PCRs were run in separate lanes on the same gel as the bestrophin PCRs, but for clarity they are shown below their respective bestrophin lanes. (B) Specificity of the dbest1 antibody. Western blot of SDS extracts from Malpighian tubules of knockout *dbest1^1-2* (KO) and *rescued* λ5; *dbest^1-2* (λ5) flies. Lanes 1 and 2 were loaded with 5 μl extract, whereas lanes 3 and 4 were loaded with 30 μl. Wild-type flies gave the same pattern as rescued flies (not depicted). (C) Western blot of S2 cell extracts from cells treated with control dsRNA (CON), dbest1 (1S), or dbest2 (2S) RNAi. Blot was probed with dbest1 antibody. (D) S2 CaC currents recorded at +100 mV $\sim$5 min after currents reached their plateau level in control cells and cells treated with RNAi as indicated. Numbers above bars indicate number of cells studied.

S2 Cells Express Four Bestrophins

To determine whether S2 cells express bestrophins, RT-PCR was performed with primers spanning exon–exon boundaries. Using several different sets of
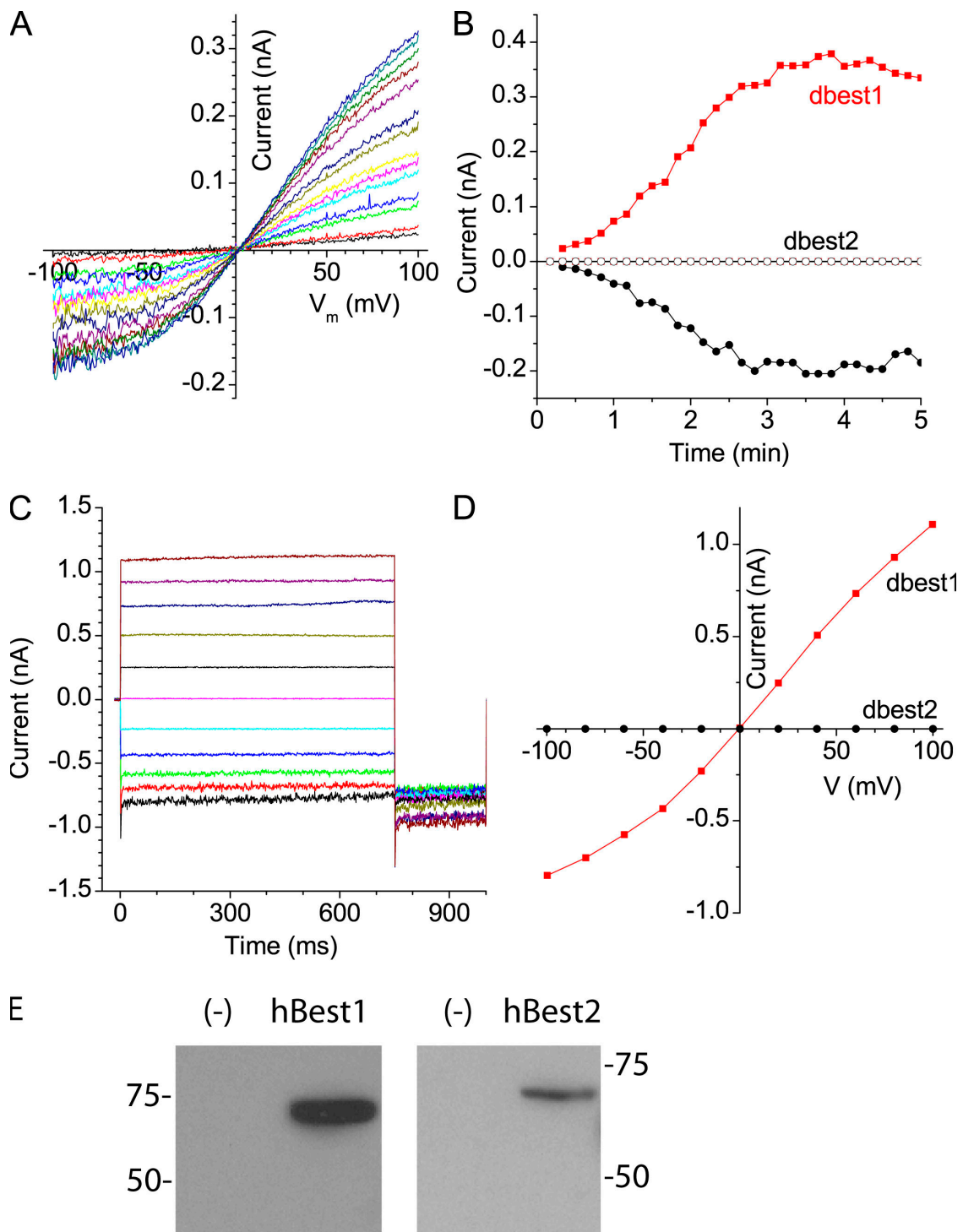
Figure 4. Expression of dbest1 and dbest2 in HEK cells. (A) Currents in HEK cells expressing dbest1 in response to voltage ramps delivered once every 10 s after patch break as in Fig. 1 A. (B) Activation of CaC current after patch break in HEK cells expressing dbest1 (filled symbols) or dbest2 (open symbols) at +100 mV (squares) and −100 mV (circles). (C) Cl currents in cells expressing dbest1 induced by step voltages between −100 mV and +100 mV at 20-mV intervals. (D) I-V curve from step protocols. (E) Endogenous expression of human bestrophins in HEK cells. Western blots using extracts from untransfected (−) HEK cells and HEK cells transfected with hBest1 or hBest2 as indicated. hBest1 was detected with rabbit polyclonal antibody A5045 made against a hBest1 C-terminal peptide. hBest2 was detected with rabbit polyclonal antibody HART4, which was made against a fusion protein of the C terminus of mouse Best2.
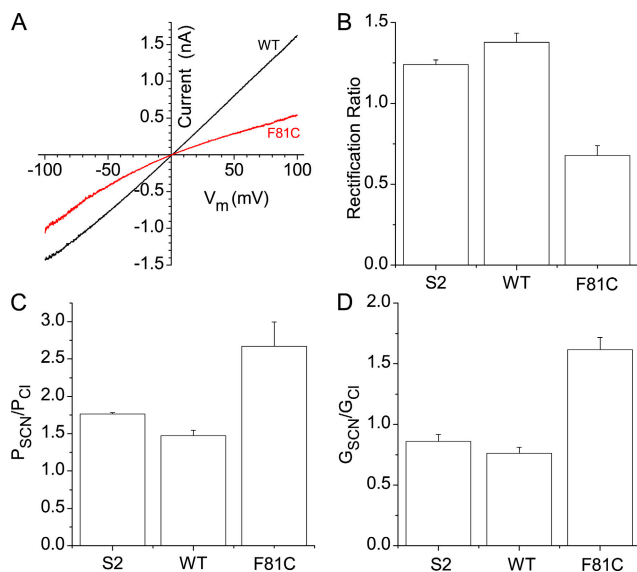
Figure 5. Effect of mutagenesis of dbest1 F81 to cysteine. (A) I-V curves from voltage ramps for wild-type and F81C dbest1 in HEK cells. (B–D) Comparison of the electrophysiological properties of endogenous S2 CaC currents with wild-type dbest1 and F81C dbest1 expressed in HEK cells. (B) Rectification ratio calculated by dividing the amplitude of the current at $+100$ mV by the absolute value of the current at -100 mV. (C) Permeability and (D) conductance of SCN relative to Cl for native S2 cells and HEK cells expressing wild-type (WT) or F81C dbest1.

primers, we amplified transcripts for four *Drosophila* bestrophins, dbest1 (AAR99659), dbest2 (AAF50668), dbest3 (AAF49648), and dbest4 (AAF49649) (Fig. 2 B). The sequences of the PCR products matched Genbank/EMBL/DDBJ sequences.

Endogenous S2 CaC Currents Are Abolished by Bestrophin-targeted RNAi

To test whether the S2 CaC current was mediated by bestrophins, we used RNAi. The first experiment was aimed at interfering nonselectively with all bestrophins. Bestrophin homologues are highly conserved in the first ~360 amino acids, but are divergent in the C termini. dsRNAs were synthesized to conserved N-terminal regions of dbest1 and dbest2 (Fig. 2 A; Table I) and mixed with the purpose of knocking down both dbest1 and dbest2. We also hoped that dbest3 and dbest4 would be reduced, because all four dbests are ~65% identical at the nucleotide level. Fig. 2 B shows the results of RT-PCR of cells treated with a mixture of the 1N and 2N dsRNAs. The transcripts for all four bestrophins were greatly reduced by RNAi treatment.

S2 cells treated with the 1N–2N dsRNAi mixture had no CaC currents (Fig. 2, C–E). Currents in RNAi-treated cells typically remained <100 pA indefinitely after breaking the patch with a high Ca^{2+} pipet solution. In contrast, currents in control cells that were treated with dsRNA to an intronic region of mBest2 were indis-

tinguishable from untreated cells as described in Fig. 1; the currents typically ran up from <100 pA to ~1 nA. Control and RNAi-treated cells were prepared from the same passage of S2 cells and patch clamped on the same day. RNAi-treated cells had no apparent morphological differences from control cells.

To determine specifically which bestrophins were responsible for the S2 CaC currents, dsRNA was made to regions of bestrophins that were divergent from one another (Fig. 2 A; Table I). Four dsRNAs were made to regions encoding parts of the unique C termini of dbest1 (1S and 1C) and dbest2 (2S and 2C). Two others were made to regions of dbest3 (3C) and dbest4 (4C) that spanned conserved and unique regions. These dsRNAs reduced or eliminated the respective transcripts (Fig. 3 A).

dbest1 protein expression was measured by Western blot using an antibody developed against a fusion protein containing amino acids 440–718 of dbest1. To test whether the antibody was specific for dbest1, we compared immunoblots from flies in which the *dbest1* gene was completely removed by recombination (*dbest1^{1-2}* line, Tavsanli et al., 2001) with flies in which the knockout was rescued by a transposon containing an 18-kb genomic fragment encompassing the entire *dbest1* gene ($\lambda 5$; *dbest1^{1-2}* line, Tavsanli et al., 2001). The antibody recognized a band near the predicted size (79.6 kD) in rescued (Fig. 3 B) and wild-type (not depicted) flies. The band was absent in the *dbest1^{1-2}* knockout flies (Fig. 3 B). These results show that the antibody was specific for dbest1 protein. In the S2 cells, a single dbest1 band was observed in cells treated with control RNAi and with dbest2-2S RNAi (Fig. 3 C). The dbest1 band was absent in S2 cells treated with dbest1-1S RNAi (Fig. 3 C). Because high-quality antibodies are not available for other *Drosophila* bestrophins, we were not able to assess effects of the other bestrophin RNAi constructs on protein levels. RNAi to dbest4 had inconsistent effects on dbest4 mRNA levels (unpublished data).

Each of the four RNAi constructs to dbest1 and dbest2 abolished CaC currents (Fig. 3 D). In Fig. 3 D, the final current amplitudes ~5 min after patch break are shown. However, in all cases, the current immediately after patch break was ~100 pA. In contrast to the absence of currents in cells treated with any of the dbest1 or dbest2 RNAi constructs, the RNAi constructs to dbest3 and dbest4 had no effect on CaC currents. The observation that the endogenous CaC current was significantly reduced by either dbest1 or dbest2 RNAi suggests that the current is composed of both dbest1 and dbest2 subunits.

Heterologous Expression of *Drosophila* Bestrophins in HEK-293 Cells

To test further whether *Drosophila* bestrophins are responsible for the S2 CaC current, HEK-293 cells were
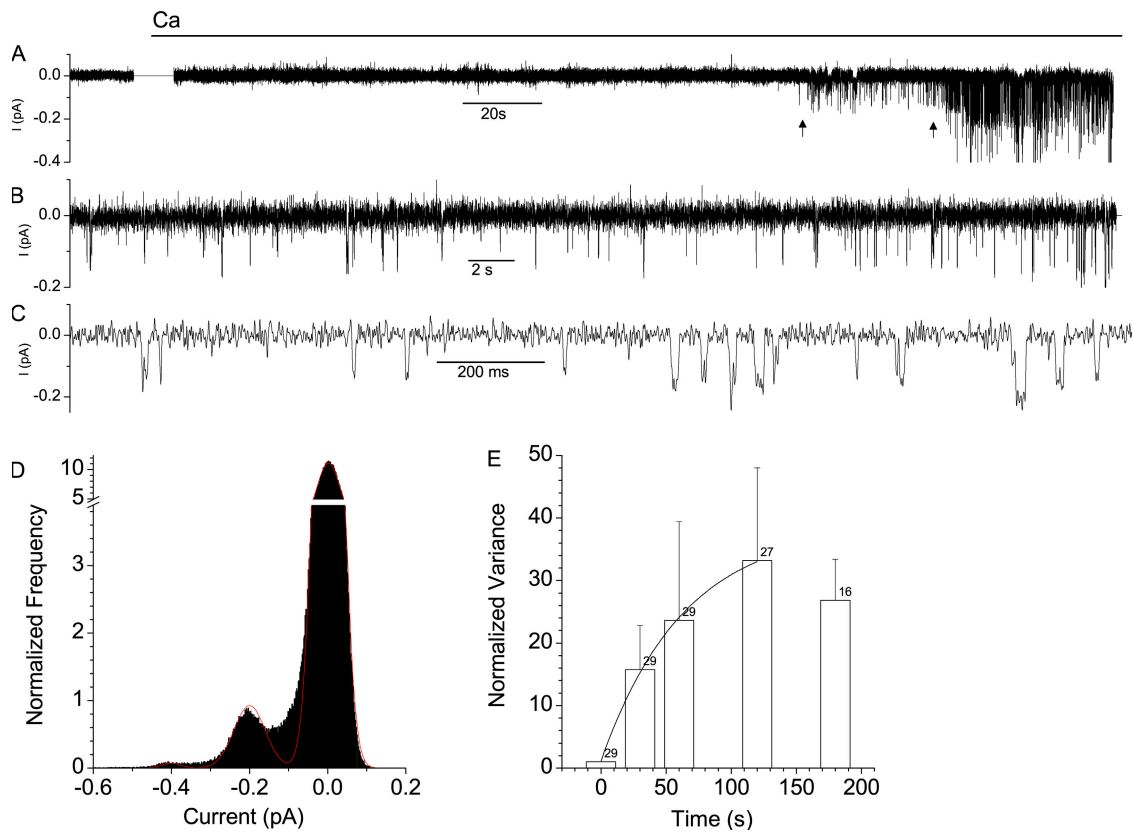
Figure 6. Single channel analysis of S2 bestrophin currents. (A) An inside-out excised patch was pulled from an S2 cell into 0 Ca^{2+} solution. During the break in the record, the solution was switched to one containing 650 nM free Ca. (B and C) Segments of the trace in A shown at higher time base as indicated. (D) All points histogram of the portion of the record in A between the arrows. (E) Time course of development of the current after addition of Ca^{2+}. The current variance was calculated for 10-s segments of records from 29 patches at various times after Ca^{2+} addition.

transiently transfected with cDNAs encoding dbest1 or dbest2. Sun et al. (2002) have previously expressed dbest1 in HEK cells and showed that it induced Cl currents. In addition, we find that transfection of HEK cells by dbest1 alone reproduced the key characteristics of the endogenous CaC current in S2 cells. (a) The current activated slowly upon patch break with a half-time of ∼2 min (Fig. 4, A and B). (b) The current had a characteristic "S" shaped I-V curve (Fig. 4, A and D). (c) The current was time independent and exhibited high current noise at negative membrane potentials (Fig. 4 C). (d) The permeability and conductance of SCN^- relative to Cl^- (P_{SCN}/P_{Cl} and G_{SCN}/G_{Cl}) were the same for the dbest1 current expressed in HEK cells and the endogenous S2 cell current (Fig. 5, B and C). P_{SCN}/P_{Cl} and G_{SCN}/G_{Cl} of dbest1 was different than what we have reported for wild-type mBest2 (Qu et al., 2004a) probably because there are four amino acids that we have shown are important in anion permeation in mBest2 that are different in dbest1. T87, L88, V89, and H91 in mBest2 are S88, I89, M90, and T92 in dbest1.

Somewhat surprisingly, expression of dbest2 alone did not induce a current (Fig. 4, B and D). However, a mixture of dbest1 and dbest2 produced currents that were similar to those produced by dbest1 alone (not depicted). The explanation for finding that dbest1 alone is sufficient to recapitulate the S2 current in HEK cells but that dbest1 and dbest2 RNAi abolish the S2 current is unknown. It is possible that dbest2 is not expressed or properly trafficked to the plasma membrane, but because we do not have an antibody for dbest2, this cannot be tested. Another possibility is that there is an endogenous bestrophin in HEK cells that can form a functional channel with dbest1 but not with dbest2. However, HEK cells do not express hbest1 or hbest2 (Fig. 4 E).

Mutagenesis Alters the Properties of dbest1 Currents

To verify that the CaC currents in dbest1-expressing HEK cells were mediated by dbest1 and not by an up-regulated endogenous channel, we changed phenylalanine 81 to cysteine (F81C) and examined the effect on the current. F81C was chosen because mutation of the homologous amino acid (F80) in mBest2 alters conductance and permeability (Qu and Hartzell, 2004). The F81C current inwardly rectified, in contrast to wild-type
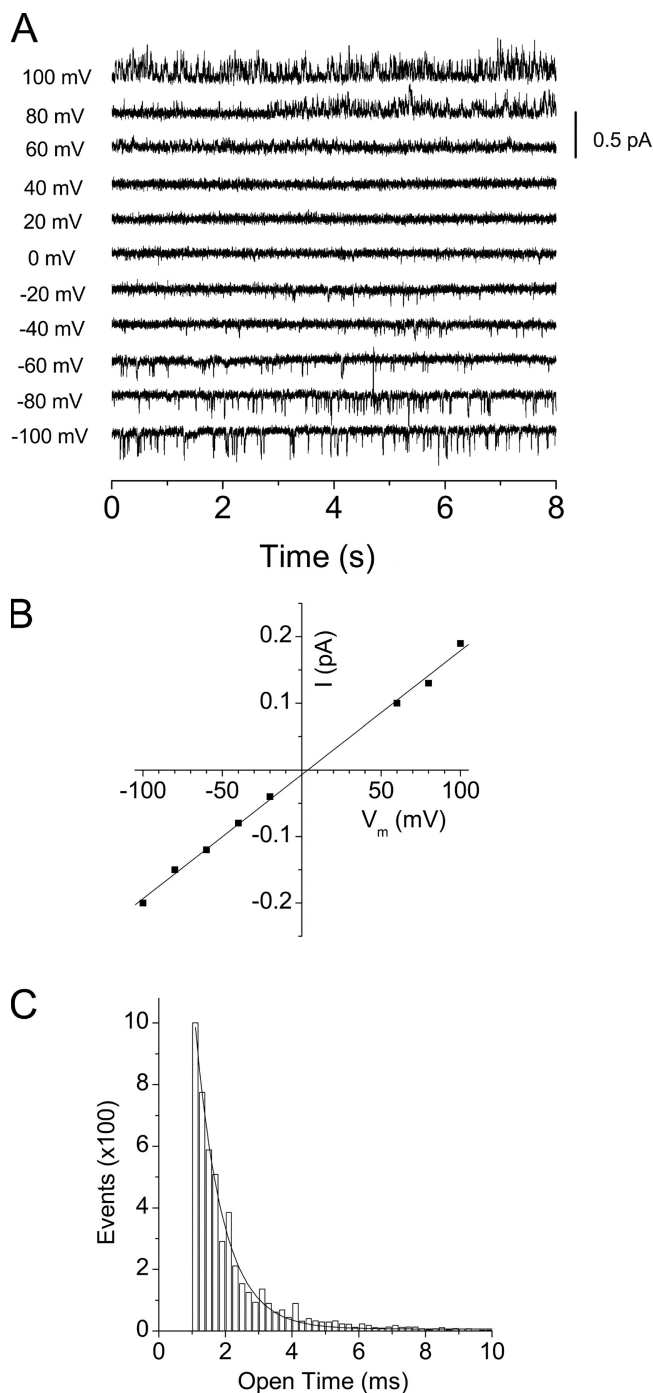
A

100 mV
80 mV
60 mV
40 mV
20 mV
0 mV
-20 mV
-40 mV
-60 mV
-80 mV
-100 mV

0.5 pA

0   2   4   6   8

Time (s)

B

I (pA)

0.2
0.1
-0.1
-0.2

-100   -50   50   100

V_m (mV)

C

Events (x100)

10
8
6
4
2
0

0   2   4   6   8   10

Open Time (ms)

Figure 7. Open time and single channel I-V curve. (A) Current traces of single S2 channel at different voltages as indicated. (B) Single channel I-V relationship. (C) Mean single channel open time obtained from a patch that contained approximately three channels that had sufficiently low open probability to permit measurement of channel open time.

dbest1 and endogenous S2 currents (Fig. 5, A and B). Also, both P_{SCN}/P_{Cl} and G_{SCN}/G_{Cl} were increased by the F81C mutation (Fig. 5, C and D). The changes in dbest1 currents resulting from the mutagenesis supports the hypothesis that the currents were mediated by dbest1.

Single-channel Analysis of *Drosophila* Bestrophin Currents

Having clearly identified the S2 CaC currents as being mediated by bestrophins, we set out to determine their single channel properties. A typical record of S2 bestrophin channels are shown in Fig. 6. Membrane patches were excised from S2 cells into 0 Ca^{2+} solution and held at $V_m = -80$ mV. After ∼20 s, the patch was switched to solution that contained Ca^{2+}. In the example, the channels did not start to become active until ∼2 min after adding Ca^{2+} (Fig. 6 A). Traces of this initial period of channel activation at higher sweep speed reveal individual channels with amplitudes of about -0.2 pA (Fig. 6, B and C). The all-points histogram (Fig. 6 D) of this part of the trace shows peaks at -0.2, -0.4, and -0.6 pA, which is consistent with at least three channels being active in the patch. After an additional 30–40 s in Ca^{2+}-containing solution, more channels became active and it was not possible to clearly resolve individual events.

Ca^{2+} stimulated channel activity significantly in 29/32 patches. In some patches, the channel was present before adding Ca^{2+}, but the open probability was low and the channel usually disappeared after 1–2 min in zero Ca^{2+} solution. Most patches contained >10 channels, so that isolated openings were resolved only during the initial period of activation. In about a third of the patches, it was not possible to resolve individual openings because too many channels were activated at once. But, even under these conditions, all-points histograms exhibited peaks separated by 0.15 to 0.2 pA at -80 mV, suggesting that the same unitary event was responsible for the activity that was observed.

The time course of channel activation was relatively slow, as suggested by the record in Fig. 6 A. To quantify the time course of activation, the variance of the current was measured at different times after introducing Ca^{2+} and normalized to the variance before adding Ca^{2+} (Fig. 6 E). The variance increased with a half-time of 63 s. This half-time was faster than we observed for the whole-cell currents in Fig. 1 (∼2 min). However, the activation of the whole cell currents was measured in cells with no ATP in the internal solution, whereas excised patches were exposed to solutions that contained 3 mM ATP. In whole cell experiments, if ATP was added to the internal solution, the activation of the whole-cell current was accelerated approximately two-fold (unpublished data). In excised patch experiments, channels were activated in only a small fraction of patches that were exposed to high Ca^{2+} without ATP in a 5-min time frame. This suggests that channel activation may involve other steps in parallel or series with Ca^{2+} binding.

The single channel exhibited a linear I-V relationship (Fig. 7, A and B). This is different from the
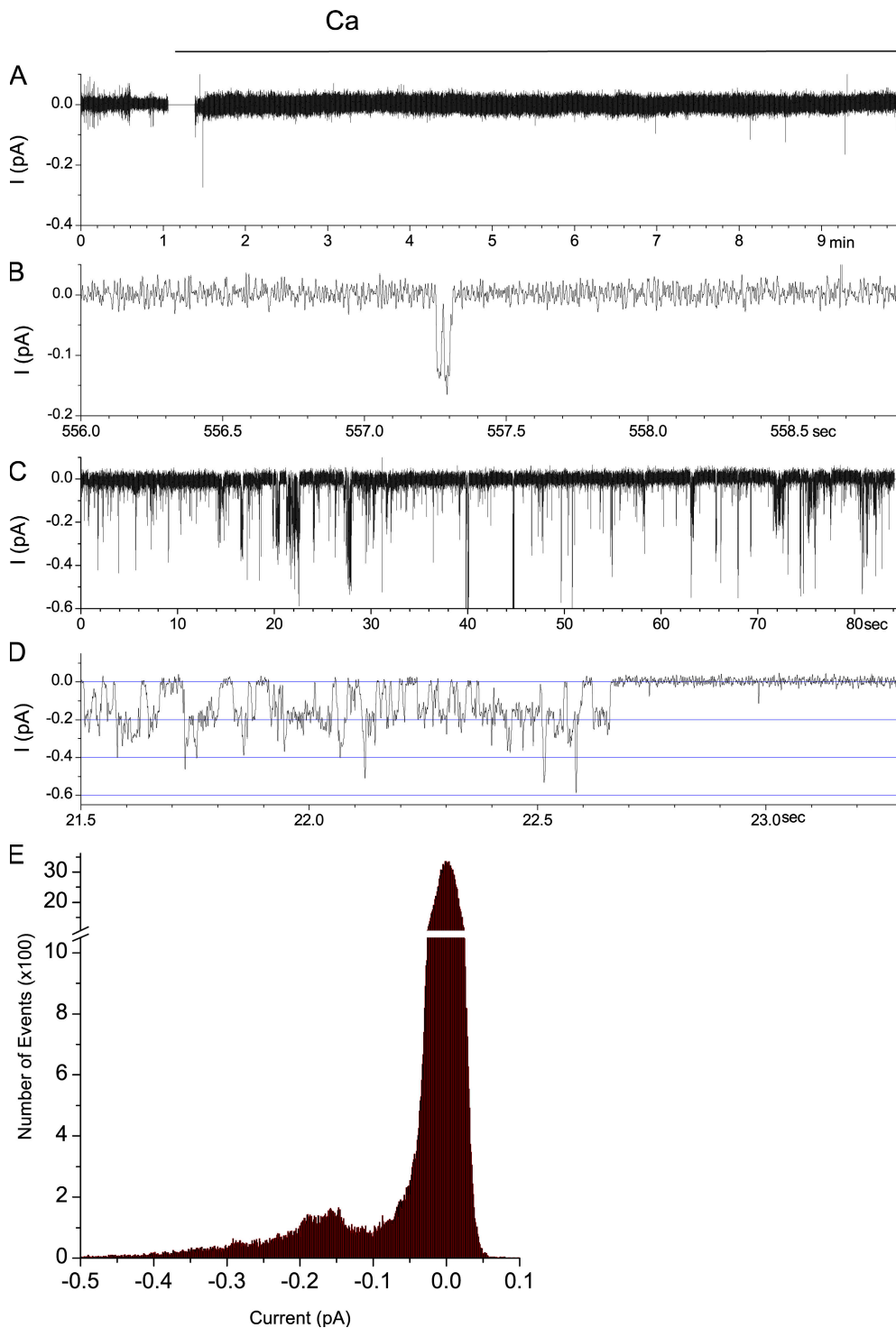
Figure 8. Single channels in S2 cells treated with dBest1 1C RNAi and in CHO cells expressing dbest1. (A) An inside-out patch was excised from an S2 cell treated with RNAi into 0 Ca^{2+} solution. During the break in the record, the patch was switched to solution containing 650 nM free Ca^{2+}. A few single channel openings can be seen. (B) Single channel opening from A shown on a faster time base. (C) Single channels in an inside-out excised patch exposed to 650 nM Ca^{2+} solution from a cell transfected with dbest1. (D) A portion of the trace in C shown on a faster time base. (E) All points histogram of the trace in C.

sigmoid I-V relationship observed for the whole-cell S2 current, suggesting that the sigmoid nature of the whole cell current was related to channel gating. It was not practical to investigate channel gating quantitatively, however, because of the presence of multiple channels in the patch, the small size of the channels, and the short single channel open time. We estimated single channel open time in patches containing a few

channels. Because it was necessary to filter the records at 200–300 Hz for analysis, channel open dwell times <1 ms were discarded. A fit of these data to a single exponential estimated a mean open time of ~1 ms at −80 mV.

To be certain that these channels were due to dbest1, we excised membrane patches from cells that had been treated with RNAi to dbest1 (1C) as in Fig. 3. The 2pS

channels described in Fig. 6 and 7 were rarely observed in patches from cells that were treated with RNAi to dbest1 (1C) (Fig. 8, A and B). In the example in Fig. 8, a few channel openings can be seen, showing that this patch was not simply an empty patch or a vesicle. Cells that were treated with control dsRNA had channels like those shown in Figs. 6 and 7.

As additional evidence that these channels are due to dbest1 expression, membrane patches were excised from CHO cells that had been transfected with dbest1 cDNA (Fig. 8, C–E). Single channels of ∼2 pS conductance were observed in patches bathed in high Ca^{2+} solution. Similar channels were also observed in patches bathed in 0 Ca^{2+} solution, but at lower frequency. Fig. 8 D illustrates a feature of the gating of these channels that was typical both of the dbest1 channels in CHO cells and in native S2 cells. The channels appeared to gate in a cooperative fashion. During the burst at the start of the record in Fig. 8 D, three different levels of opening are evident (0.17, 0.34, and 0.51 pA; Fig. 8 E). The burst then ends and there are no channel openings for several seconds. In some records, this bursting activity seemed to involve as many as five individual channels, although quantitative analysis of these multichannel bursts was difficult. In any case, the results with RNAi treatment of S2 cells and overexpression of dbest1 in CHO cells provide strong arguments that these channels are responsible for the whole-cell bestrophin current in S2 cells.

DISCUSSION

The experiments in this paper add considerable strength to the hypothesis that bestrophins are indeed Ca^{2+}-activated Cl^- channels. The observation that we can abolish the native S2 CaC current with several different dsRNA constructs directed against dbest1 or dbest2, but not dbest3 or dbest4 is unambiguous evidence that bestrophins are essential components of CaC channels. Although this alone does not prove that bestrophins form the pore of the channel, the demonstration that expression of dbest1 in HEK cells induces a current with the same characteristics as the endogenous S2 CaC current and that mutation of F81 alters the rectification properties and P_{SCN}/P_{Cl} and G_{SCN}/G_{Cl} of the current lends additional confidence to the conclusion.

The single channel properties of bestrophin currents have not previously been reported. The single channels that we describe here have a single channel conductance of 2 pS, a value that is similar to other CaC channels that have been studied in *Xenopus* oocytes (Takahashi et al., 1987), cardiac myocytes (Collier et al., 1996), arterial smooth muscle (Klockner, 1993; Hirakawa et al., 1999; Piper and Large, 2003), A6 kidney cells (Marunaka and Eaton, 1990), and endocrine cells (Taleb et al., 1988; Ho et al., 2001). Our channels have properties that, at least superficially, are remarkably similar to CaC channels that have been studied in arterial smooth muscle (Piper and Large, 2003) and endocrine cells (Ho et al., 2001).

Recently, Tsunenari et al. (2006) have described macroscopic CaC currents in inside out patches excised from cells expressing hBest4. Interestingly, these channels activated slowly after addition of Ca^{2+} to the cytosolic face of the patch. At saturating Ca^{2+} concentrations of 10 μM, the channels activated with a time constant of ∼15 s. This is several fold faster than we find for dbest1, but the kinetics of activation of different bestrophins may be different. For example, mBest2 expressed in HEK cells is activated very quickly after patch break (<10 s), whereas dbest1 requires ∼2 min for complete activation. As Tsunenari et al. point out, the mechanism of this slow activation is unknown, but is unlikely to be due to direct binding of Ca^{2+} to the channel. Clearly, an important question for future investigations will be the mechanisms of activation of bestrophin channels.

REFERENCES

Allikmets, R., J.M. Seddon, P.S. Bernstein, A. Hutchinson, A. Atkinson, S. Sharma, B. Gerrard, W. Li, M.L. Metzker, C. Wadelius, et al. 1999. Evaluation of the Best disease gene in patients with age-related macular degeneration and other maculopathies. *Hum. Genet.* 104:449–453.

Attali, B., E. Guillemare, F. Lesage, E. Honore, G. Romey, M. Lazdunski, and J. Barhanin. 1993. The protein IsK is a dual activator of K^+ and Cl^- channels. *Nature.* 365:850–852.

Bakall, B., L.Y. Marmorstein, G. Hoppe, N.S. Peachey, C. Wadelius, and A.D. Marmorstein. 2003. Expression and localization of bestrophin during normal mouse development. *Invest. Ophthalmol. Vis. Sci.* 44:3622–3628.

Clapham, D. 1998. The list of potential volume-sensitive chloride currents continues to swell (and shrink). *J. Gen. Physiol.* 111:623–624.

Collier, M.L., P.C. Levesque, J.L. Kenyon, and J.R. Hume. 1996. Unitary Cl^- channels activated by cytoplasmic Ca^{2+} in canine ventricular myocytes. *Circ. Res.* 78:936–944.

Cross, H.E., and L. Bard. 1974. Electro-oculography in Best's macular dystrophy. *Am. J. Ophthalmol.* 77:46–50.

Cunningham, S.A., M.S. Awayda, J.K. Bubien, I.I. Ismailov, M.P. Arrate, B.K. Berdiev, D.J. Benos, and C.M. Fuller. 1995. Cloning of an epithelial chloride channel from bovine trachea. *J. Biol. Chem.* 270:31016–31026.

Deutman, A.F. 1969. Electro-oculography in families with vitelliform dystrophy of the fovea. Detection of the carrier state. *Arch. Ophthalmol.* 81:305–316.

Eggermont, J. 2004. Calcium-activated chloride channels: (un)known, (un)loved? *Proc. Am. Thorac. Soc.* 1:22–27.

Gallemore, R.P., B.A. Hughes, and S.S. Miller. 1997. Retinal pigment epithelial transport mechanisms and their contributions to the electroretinogram. *Prog. Retinal Eye Res.* 16:509–566.

Gibson, A., A.P. Lewis, K. Affleck, E. Meldrum, and N. Thompson. 2005. hCLCA1 and mCLCA3 are secreted non-integral membrane proteins and therefore are not ion channels. *J. Biol. Chem.* 280:27205–27212.

Godel, V., G. Chaine, L. Regenbogen, and G. Coscas. 1986. Best's vitelliform macular dystrophy. *Acta Ophthalmol. Suppl.* 175:1–31.

Hartzell, C., I. Putzier, and J. Arreola. 2005a. Calcium-activated chloride channels. *Annu. Rev. Physiol.* 67:715–758.

Hartzell, C., Z. Qu, I. Putzier, L. Artinian, L.-T. Chien, and Y. Cui. 2005b. Looking chloride channels straight in the eye: bestrophins, lipofuscinosis, and retinal degeneration. *Physiology.* 20:292–302.

Hirakawa, Y., M. Gericke, R.A. Cohen, and V.M. Bolotina. 1999. Ca^{2+}-dependent Cl^- channels in mouse and rabbit aortic smooth muscle cells: regulation by intracellular Ca^{2+} and NO. *Am. J. Physiol.* 277:H1732–H1744.

Ho, M.W., M.A. Kaetzel, D.L. Armstrong, and S.B. Shears. 2001. Regulation of a human chloride channel. a paradigm for integrating input from calcium, type II calmodulin-dependent protein kinase, and inositol 3,4,5,6-tetrakisphosphate. *J. Biol. Chem.* 276:18673–18680.

Jentsch, T.J., V. Stein, F. Weinreich, and A.A. Zdebik. 2002. Molecular structure and physiological function of chloride channels. *Physiol. Rev.* 82:503–568.

Klockner, U. 1993. Intracellular calcium ions activate a low-conductance chloride channel in smooth-muscle cells isolated from human mesenteric artery. *Pflugers Arch.* 424:231–237.

Kramer, F., K. White, D. Pauleikhoff, A. Gehrig, L. Passmore, A. Rivera, G. Rudolph, U. Kellner, M. Andrassi, B. Lorenz, et al. 2000. Mutations in the VMD2 gene are associated with juvenile-onset vitelliform macular dystrophy (Best disease) and adult vitelliform macular dystrophy but not age-related macular degeneration. *Eur. J. Hum. Genet.* 8:286–292.

Linsenmeier, R.A., and R.H. Steinberg. 1982. Origin and sensitivity of the light peak in the intact cat eye. *J. Physiol.* 331:653–673.

Marmorstein, A.D., L.Y. Mormorstein, M. Rayborn, X. Wang, J.G. Hollyfield, and K. Petrukhin. 2000. Bestrophin, the product of the Best vitelliform macular dystrophy gene (VMD2), localizes to the basolateral membrane of the retinal pigment epithelium. *Proc. Natl. Acad. Sci. USA.* 97:12758–12763.

Marmorstein, A.D., J.B. Stanton, J. Yocom, B. Bakall, M.T. Schiavone, C. Wadelius, L.Y. Marmorstein, and N.S. Peachey. 2004. A model of best vitelliform macular dystrophy in rats. *Invest. Ophthalmol. Vis. Sci.* 45:3733–3739.

Marmorstein, L.Y., J. Wu, P. McLaughlin, J. Yocom, M.O. Karl, R. Neussert, S. Wimmers, J.B. Stanton, R.G. Gregg, O. Strauss, et al. 2006. The light peak of the electroretinogram is dependent on voltage-gated calcium channels and antagonized by bestrophin (Best-1). *J. Gen. Physiol.* 127:577–589.

Marquardt, A., H. Stohr, L.A. Passmore, F. Krämer, A. Rivera, and B.H. Weber. 1998. Mutations in a novel gene, VMD2, encoding a protein of unknown properties cause juvenile-onset vitelliform macular dystrophy (Best's disease). *Hum. Mol. Genet.* 7:1517–1525.

Marunaka, Y., and D.C. Eaton. 1990. Effects of insulin and phosphatase on a Ca^{2+}-dependent Cl^- channel in a distal nephron cell line (A6). *J. Gen. Physiol.* 95:773–789.

Mehta, A. 2005. CFTR: more than just a chloride channel. *Pediatr. Pulmonol.* 39:292–298.

Penfold, P.L., M.C. Madigan, M.C. Gillies, and J.M. Provis. 2001. Immunological and aetiological aspects of macular degeneration. *Prog. Retin. Eye Res.* 20:385–414.

Petrukhin, K., M.J. Koisti, B. Bakall, W. Li, G. Xie, T. Marknell, O. Sandgren, K. Forsman, G. Holmgren, S. Andreasson, et al. 1998. Identification of the gene responsible for Best macular dystrophy. *Nat. Genet.* 19:241–247.

Piper, A.S., and W.A. Large. 2003. Multiple conductance states of single Ca^{2+}-activated Cl^- channels in rabbit pulmonary artery smooth muscle cells. *J. Physiol.* 547:181–196.

Pollack, K., F.R. Kreuz, and L.E. Pillunat. 2005. Best's disease with normal EOG. Case report of familial macular dystrophy. *Ophthalmologe.* 102:891–894.

Pusch, M. 2004. Ca(2+)-activated chloride channels go molecular. *J. Gen. Physiol.* 123:323–325.

Qu, Z., and H.C. Hartzell. 2000. Anion permeation in Ca^{2+}-activated Cl^- channels. *J. Gen. Physiol.* 116:825–844.

Qu, Z., and H.C. Hartzell. 2003. Two bestrophins cloned from *Xenopus laevis* oocytes express Ca-activated Cl currents. *J. Biol. Chem.* 278:49563–49572.

Qu, Z., and H.C. Hartzell. 2004. Determinants of anion permeation in the second transmembrane domain of the mouse bestrophin-2 chloride channel. *J. Gen. Physiol.* 124:371–382.

Qu, Z., L.-T. Chien, Y. Cui, and H.C. Hartzell. 2006a. The anion-selective pore of the bestrophins, a family of chloride channels associated with retinal degeneration. *J. Neurosci.* 26:5411–5419.

Qu, Z., Y. Cui, and C. Hartzell. 2006b. A short motif in the C-terminus of mouse bestrophin 4 inhibits its activation as a Cl channel. *FEBS Lett.* 580:2141–2146.

Q u, Z., R. Fischmeister, and H.C. Hartzell. 2004. Mouse bestrophin-2 is a bona fide Cl^- channel: identification of a residue important in anion binding and conduction. *J. Gen. Physiol.* 123:327–340.

Renner, A.B., H. Tillack, H. Kraus, F. Kramer, N. Mohr, B.H. Weber, M.H. Foerster, and U. Kellner. 2005. Late onset is common in best macular dystrophy associated with VMD2 gene mutations. *Ophthalmology.* 112:586–592.

Rosenthal, R., B. Bakall, T. Kinnick, N. Peachey, S. Wimmers, C. Wadelius, A. Marmorstein, and O. Strauss. 2005. Expression of bestrophin-1, the product of the VMD2 gene, modulates voltage-dependent Ca^{2+} channels in retinal pigment epithelial cells. *FASEB J.* 20:178–180.

Seddon, J.M., S. Sharma, S. Chong, A. Hutchinson, R. Allikmets, and R.A. Adelman. 2003. Phenotype and genotype correlations in two best families. *Ophthalmology.* 110:1724–1731.

Seddon, J.M., M.A. Afshari, S. Sharma, P.S. Bernstein, S. Chong, A. Hutchinson, K. Petrukhin, and R. Allikmets. 2001. Assessment of mutations in the best macular dystrophy (VMD2) gene in patients with adult-onset foveomacular vitelliform dystrophy, age-related maculopathy, and bull's-eye maculopathy. *Ophthalmology.* 108:2060–2067.

Shimbo, K., D.L. Brassard, R.A. Lamb, and L.H. Pinto. 1995. Viral and cellular small integral membranes proteins can modify ion channels endogenous to *Xenopus* oocytes. *Biophys. J.* 69:1819–1829.

Strauss, O. 2005. The retinal pigment epithelium in visual function. *Physiol. Rev.* 85:845–881.

Sun, H., T. Tsunenari, K.-W. Yau, and J. Nathans. 2002. The vitelliform macular dystrophy protein defines a new family of chloride channels. *Proc. Natl. Acad. Sci. USA.* 99:4008–4013.

Takahashi, T., E. Neher, and B. Sakmann. 1987. Rat brain serotonin receptors in *Xenopus* oocytes are coupled by intracellular calcium to endogenous channels. *Proc. Natl. Acad. Sci. USA.* 84:5063–5067.

Taleb, O., P. Feltz, J.L. Bossu, and A. Feltz. 1988. Small-conductance chloride channels activated by calcium on cultured endocrine cells from mammalian pars intermedia. *Pflugers Arch.* 412:641–646.

Tavsanli, B.C., K.S. Pappu, S.Q. Mehta, and G. Mardon. 2001. Dbest1, a *Drosophila* homolog of human Bestrophin, is not required for viability or photoreceptor integrity. *Genesis.* 31:130–136.

Tsien, R.Y., and T. Pozzan. 1989. Measurements of cytosolic free Ca^{2+} with Quin-2. *Meth. Enyzmol.* 172:230–262.

Tsunenari, T., H. Sun, J. Williams, H. Cahill, P. Smallwood, K.-W. Yau, and J. Nathans. 2003. Structure-function analysis of the bestrophin family of anion channels. *J. Biol. Chem.* 278:41114–41125.

Tsunenari, T., J. Nathans, and K.W. Yau. 2006. Ca^{2+}-activated Cl$^-$ current from human bestrophin-4 in excised membrane patches. *J. Gen. Physiol.* 127:749–754.

Tzounopoulos, T., J. Maylie, and J.P. Adelman. 1995. Induction of endogenous channels by high levels of heterologous membrane proteins in *Xenopus* oocytes. *Biophys. J.* 69:904–908.

Van Gelder, R.N., M.E. von Zastrow, A. Yool, W.C. Dement, J.D. Barchas, and J.H. Eberwine. 1990. Amplified RNA synthesized from limited quantities of heterogeneous cDNA. *Proc. Natl. Acad. Sci. USA.* 87:1663–1667.

Wajima, R., S.B. Chater, O. Katsumi, M.C. Mehta, and T. Hirose. 1993. Correlating visual acuity and electrooculogram recordings in Best's Disease. *Ophthalmologica.* 207:174–181.

Weber, B.H.F., and F. Krämer. 2002. VMD2 Mutation Database. http://www. uni-wuerzburg. de/humangenetics/vmd2. html.

White, K., A. Marquardt, and B.H.F. Weber. 2000. VMD2 mutations in vitelliform macular dystrophy (Best disease) and other maculopathies. *Hum. Mutat.* 15:301–308.

Yamazaki, J., K. Okamura, K. Ishibashi, and K. Kitamura. 2005. Characterization of CLCA protein expressed in ductal cells of rat salivary glands. *Biochim. Biophys. Acta.* 1715:132–144.

Yardley, J., B.P. Leroy, N. Hart-Holden, B.A. Lafaut, B. Loeys, L.M. Messiaen, R. Perveen, M.A. Reddy, S.S. Bhattacharya, E. Traboulsi, et al. 2004. Mutations of VMD2 splicing regulators cause nanophthalmos and autosomal dominant vitreoretinochoroidopathy (ADVIRC). *Invest. Ophthalmol. Vis. Sci.* 45: 3683–3689.

Yu, K., Y. Cui, and H.C. Hartzell. 2006. The bestrophin mutation A243V, linked to adult-onset vitelliform macular dystrophy, impairs its Cl channel function. *Invest. Ophthalmol. Vis. Sci.* In press.